Structural and Vibrational Characterization of Polyaniline Nanofibers Prepared from Interfacial Polymerization

Gustavo M. do Nascimento,*,† Pedro Y. G. Kobata, and Marcia L. A. Temperini

Departamento de Química Fundamental, Instituto de Química, Universidade de São Paulo, CP 26.077, CEP 05513-970, São Paulo, SP, Brazil

Received: October 16, 2007; Revised Manuscript Received: July 30, 2008

This work deals with the structural and vibrational characterization of PANI nanofibers prepared through interfacial polymerization using different concentrations of HCl aqueous solution. The results were compared to those obtained by PANI prepared through the conventional route. X-ray diffraction and small-angle X-ray scattering techniques showed that high concentrations of HCl solutions used in the preparation of the PANI nanofibers reduce their crystallinity. The increase of regions with granular morphology was also observed in the scanning electron microscopy images. The changes in the resonance Raman spectra from 200 to 500 cm^{-1}, FTIR spectra, and the EPR data of the PANI nanofibers reveal an increase in the torsion angles of $C_{ring}-N-C_{ring}$ segments owing the formation of bipolarons in the PANI backbone higher than the PANI samples prepared by conventional route.

Introduction

The polyaniline (PANI) and its derivatives are one of the most studied conducting polymers owing to their electrochromic and photoconductivity properties allied with their higher stability in air and easier doping process, as compared to other conducting polymers.[1−3] These properties made PANI attractive for use in solar cells, displays, lightweight battery electrodes, electromagnetic shielding devices, anticorrosion coatings, and sensors.[4−7] PANI has different oxidation and protonation states;[1−3] the emeraldine oxidation state (PANI-EB) is that in which the number of reduced or benzenoid units is equal to oxidized or quinoid units. The conducting form of PANI as the emeraldine salt (PANI-ES) has benzenoid, radical cation (polaron), and dication (bipolaron) segments in its polymeric chains (see Scheme 1). For highly doped PANI, the formation of bipolaron segments are more favorable than the polaron ones.[8−10]

SCHEME 1: Representation of the Characteristic PANI Forms

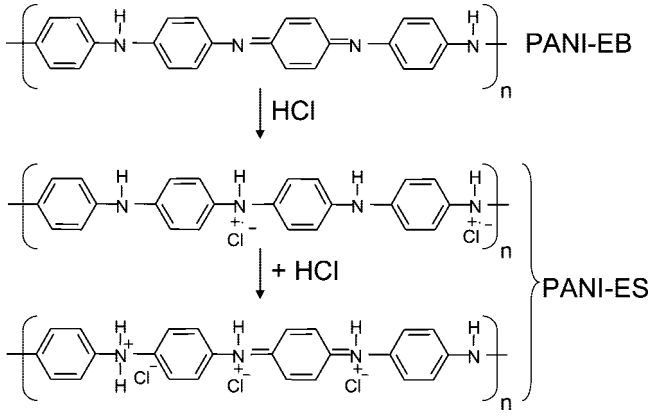

The recent research efforts are to deal with the control and the enhancement of the bulk properties of PANI, mainly by formation of organized PANI chains in blends, composites, and nanofibers.[11−15] For instance, the synthesis of nanostructured PANI, especially as nanofibers and nanotubes, can improve its electrical, thermal, and mechanical stabilities. These materials can have an important impact for application in electronic devices and molecular sensors owing their extremely high surface area, synthetic versatility, and low cost.[12]

The conventional synthesis of polyaniline, based on the oxidative polymerization of aniline in the presence of a strong acid dopant,[1−3] typically results in an irregular granular morphology that is accompanied by a very small percentage of nanoscale fibers.[16] To circumvent this behavior, several approaches have been developed by which nanofibers can be obtained as the dominant nanostructure. For instance, the nanoporous membranes have been used for the template synthesis of conducting polymers, metals, and other materials. Highly monodispersed nanofibers and tubules are subsequently obtained by dissolving the membrane template.[17,18]

In the absence of an external physical or chemical template, pure PANI nanofibers/tube can also be obtained by making use of large organic acids. These acids form micelles upon which aniline is polymerized and doped. Fiber diameters are observed to be as low as 30−60 nm and are highly influenced by reagent ratios.[19−23] Ionic liquids, organic salts that are liquid at low temperature, have also been used as synthetic media for the preparation of nanostructured PANI (specially liquids derived from the imidazolium cation).[24,25]

Uniform nanofibers of pure metallic PANI (30−120 nm diameter, depending on the dopant) have also been prepared by polymerization at an aqueous−organic interface.[16,26,27] It is hypothesized that migration of the product into the aqueous phase can suppress uncontrolled polymer growth by isolating the fibers from the excess of reagents.[16,26] It has recently been demonstrated that the addition of certain surfactants to such an interfacial system grants further control over the diameter of

* To whom correspondence should be addressed. E-mail: morari@yahoo.com.
† Present address: Department of Electrical Engineering and Computer Science, Massachusetts Institute of Technology, Cambridge, Massachusetts 02139-4307.

10.1021/jp804154k CCC: $40.75
Published on Web 08/22/2008

TABLE 1: Elemental Analysis of PANI Samples and their Molecular Formula and Cl/N Ratio

samples	%C	%H	%N	%Cl	molecular formula	Cl/N
tetramer[a]	66.2	4.63	12.9	16.3	$C_{24}H_{18}N_4 \cdot 2HCl$	0.5
ES-5M	42.5	5.65	8.22	18.4	$C_{24}H_{18}N_4 \cdot 3.5HCl \cdot 11H_2O$	0.87
IF1-5M	47.7	4.99	9.39	22.6	$C_{24}H_{18}N_4 \cdot 4HCl \cdot 6H_2O$	1.0
IF1-3M	55.3	5.28	10.1	14.7	$C_{24}H_{18}N_4 \cdot 2HCl \cdot 5H_2O$	0.5
IF1-2M	52.0	5.60	9.60	14.4	$C_{24}H_{18}N_4 \cdot 2HCl \cdot 7H_2O$	0.5
ES-1M	48.9	4.80	9.50	18.3	$C_{24}H_{18}N_4 \cdot 3HCl \cdot 6H_2O$	0.75

[a] The values for the tetramer were calculated.

the nanofibers. "Seeding" with various nanomaterials has also been used with great effect to initiate PANI nanofiber formation in single-phase polymerizations.[28,29] Thus, the template-free methods, such as interfacial, seeding, and micellar, can be employed as different "bottom-up" approaches to obtain pure PANI nanofibers. The possibility to prepare nanostructured PANI by self-assembly with reduced postsynthesis processing warrants further study and application of these materials, especially in the field of electronic nanomaterials.

The main goal of this work is the investigation of the structural and vibrational features of the PANI nanofibers prepared through interfacial polymerization using different concentrations of HCl aqueous solution. The materials were characterized by scanning electron microscopy (SEM), X-ray diffraction (XRD), small-angle X-ray scattering (SAXS), resonance Raman (RR), and electron paramagnetic resonance (EPR). The results were compared to those obtained by PANI prepared through the conventional route.

Experimental Section

a. Preparation of Poly(aniline) through Interfacial Polymerization. The experimental procedure for preparation of PANI nanofibers was adapted from refs 16 and 26. A total of 2.90 mL of aniline (MERCK, previously distillated under vacuum) was mixed with chloroform (MERCK) up to a volume of 100 mL into a beaker of 600.0 mL. Another solution having 1.83 g of $(NH_4)_2S_2O_8$ (MERCK) dissolved in 100.0 mL of 2.0 mol/L of HCl aqueous solution was slowly dropped on the wall of the beaker containing the aniline/HCl aqueous solution at room temperature. The reaction solution was kept without agitation for 24 h. Afterward, the dark green solid was filtrated and washed with 300 mL of 2.0 mol/L of HCl aqueous solution and then with 200 mL of acetone (MERCK). Using the same experimental procedure described above, the PANI was prepared using 3.0 and 5.0 mol/L of HCl aqueous solution. In this work, the polymers prepared with 2.0, 3.0, and 5.0 mol/L of HCl aqueous solution will be labeled IF1-2M, IF1-3M, and IF1-5M, respectively. Table 1 displays the elemental analysis (C, H, N, Cl) of all materials and the molecular formula (considering the tetramer of PANI as the unit cell).

b. Preparation of Poly(aniline) through Standard Procedure. The emeraldine salt form of PANI (ES-1M) was prepared according to the procedure described by MacDiarmid et al.[30] For preparing the ES-1M, it is necessary to prepare two solutions: (i) 11.5 g of solid $(NH_4)_2S_2O_8$ (MERCK) was dissolved in 200.0 mL of 1.0 mol/L of HCl aqueous solution and (ii) 20.0 mL of aniline (MERCK, previously distillated under vacuum) was added in 300 mL of 1 mol/L of HCl aqueous solution. Afterward, the solutions were refrigerated up to 2−5 °C in ice/water bath and mixed. The reaction solution was maintained at that temperature in the ice/water bath and under magnetic stirring for 1.5 h. After this period, a dark green solid was isolated by filtration, washed with 500.0 mL of 1.0 mol/L of HCl aqueous solution, and dried in a desiccator. For comparison purposes, another PANI emeraldine salt was prepared using the same procedure described above, using 5.0 mol/L HCl aqueous solution. This sample was named ES-5M (the elemental analysis is displayed in Table 1).

c. Instrumentation. The SEM images of powdered samples, dispersed over a drop of silver glue, were recorded in a Field Emission Gun (SEM, JSM-6330), operated with a high-tension voltage of 5 kV. XRD patterns of powdered samples were obtained on a Rigaku diffractometer model Miniflex using Cu Kα radiation (1.541 Å, 30 kV, 15 mA, step of 0.05°). For measuring the XRD patterns, a glass support was used (having 1 cm^2 of available area for samples and with 5 mm of thickness).

The SAXS experiments were conducted at the National Synchrotron Light Laboratory (LNLS), Campinas, Brazil, by using a monochromatic X-ray beam ($\lambda = 1.596$ Å), which also focuses the beam horizontally, and a position-sensitive X-ray detector to record the scattering intensity. The measurements were done in a cell having constant geometry and with mica windows.[31] The amount of polymer used in all measurements was at about 0.20 g to ensure the reproducibility and comparison among the curves. The parasitic scattering intensity (mainly produced by the cell windows) was subtracted from the total experimental intensity. The SAXS curves were normalized with respect to (i) the decreasing intensity of the incoming synchrotron beam and (ii) the SAXS intensity produced by air (cell with mica windows without sample), which was measured and subtracted from the total scattering intensity before the analysis.

Raman spectra were acquired on a Renishaw Raman Imaging Microscope System 3000 equipped with a charge-coupled-device (CCD) detector and coupled to an Olympus metallurgical microscope (BH2-UMA), which allowed rapid accumulation of Raman spectra with spatial resolution of about 1 μm (micro-Raman technique). The calibration of the equipment (wavenumbers and intensities of the peaks) was done using a Si monocrystalline sample. The laser beam was focused on the sample with an 80× lens. The laser power was always kept below 0.02 mW at the sample to avoid its thermal and photochemical degradation. Experiments were performed under room conditions with a backscattering geometry. Samples were irradiated with the 632.8 nm line of a He−Ne laser (Coherent).

UV−vis-NIR spectra of PANI powdered samples dispersed in Nujol mineral oil were obtained in Shimadzu UVPC-3101 scanning spectrophotometer in transmission mode.

FTIR spectra were obtained by using a BOMEM MB-100 instrument with a resolution of 4 cm^{-1}, and the samples were dispersed in KBr pellets. To better observe the spectral features, mainly for those observed at regions higher than 2500 cm^{-1}, a baseline correction was used. The baseline correction (multiple point level, 10 points used) was done using the Grams/386 software for all FTIR data. The original data are displayed (see Supporting Information) for two samples and it is possible to observe that the baseline was done to maintain the relative intensities among the bands.

EPR spectra of powdered samples were recorded in a Bruker EMX instrument, operating at X-band frequency (~9.5 GHz), at room temperature, using DPPH (α,α′-biphenyl-β-picrylhydrazyl) as frequency calibrant ($g = 2.0036$). The amount of polymer used in each measurement was at about 0.010 g to ensure the comparison between the spectra. Elemental analysis were performed in a Perkin-Elmer CHN 2400.

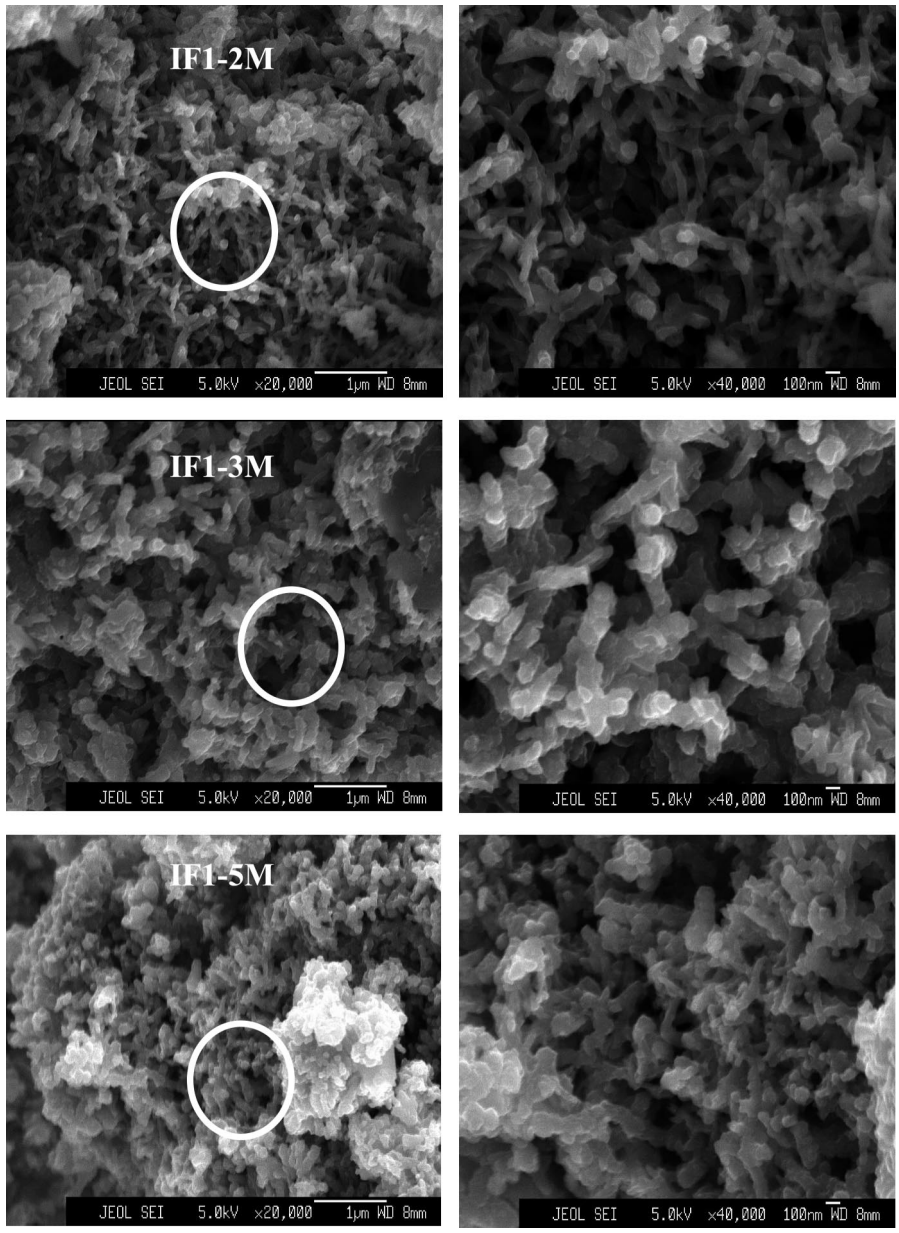

Figure 1. SEM images of powdered samples of IF1-2M (A), IF1-3M (B), and IF1-5M (C).

Results and Discussion

Figure 1 shows the SEM images obtained for PANI prepared by interfacial polymerization. The presence of fibers was clearly observed in all images (the fibers were not observed for ES-1M, images not shown). The images are presented in two magnifications (20000× and 40000×), where in the lower ones it was possible to see that the fiber morphology is dominant and in the higher ones it was possible to estimate that the diameter of the nanofibers is approximately 30 nm. Our results are in agreement with the previous data obtained by Huang et al.[16,26] The authors demonstrated that only using concentrations of acid higher than 1 mol/L it was possible to obtain nanofibers with high quality. However, for IF1-5M sample there was observed a decrease in the amount of nanofibers and more regions with irregular morphology as compared to other IF1 samples. This result reveals that high HCl concentrations damage the nanofiber morphology of PANI. Considering the results obtained by Kaner et al.,[16,26] just synthetic media with HCl concentrations varying from 1 to 3 mol/L, it was possible to obtain nanofibers of PANI with high quality.

Figure 2 shows the X-ray diffraction pattern of PANI samples. For PANI prepared through standard procedure (ES-1M) the XRD pattern corresponds to that observed in the literature for PANI type-I (pseudo-orthorhombic unit cell), according to Pouget et al.[32] The XRD patterns for IF1 samples have the same peaks observed for ES-1M, indicating that all samples are type-I. However, it was observed that the samples IF1-2M and IF1-3M have more intense signal (see Figure 2) than other samples, indicating more crystallinity. Another evidence of higher crystallinity was the presence of peaks with higher d values (higher than 1.0 nm, see Figure 2). The presence of peaks at low angles (or high distance) can be clearly observed in SAXS curves (see Figure 3), where the statistics at low angles are better than the conventional XRD data, of IF1-2M and IF1-3M samples. Thus, the acid concentration used in the interfacial polymerization can modulate the degree of crystallinity and quality of nanofibers obtained.

The Raman spectra at 632.8 nm (from 600 to 1700 cm^{-1}) of IF1 samples show similar profiles to that observed for ES-1M (see Figure 4). The bands at about 1163 cm^{-1} (βC—H) and

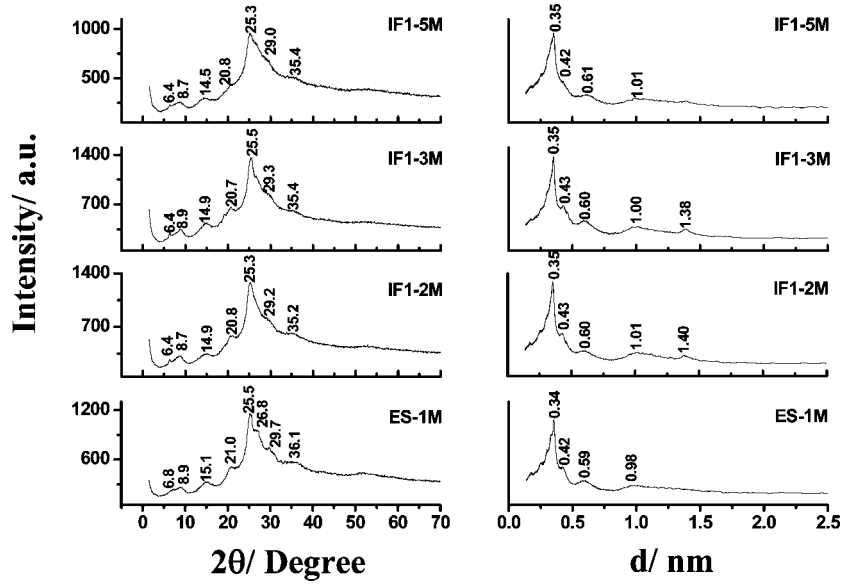

Figure 2. X-ray diffractograms of powdered samples of ES-1M, IF1-2M, IF1-3M, and IF1-5M.

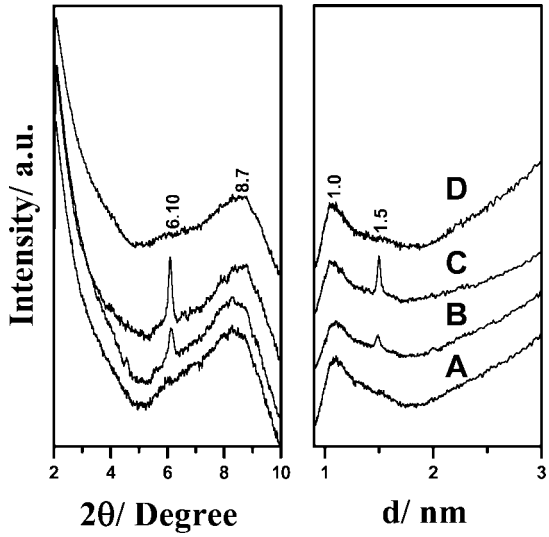

Figure 3. SAXS curves of powdered samples of ES-1M (A), IF1-2M (B), IF1-3M (C), and IF1-5M (D).

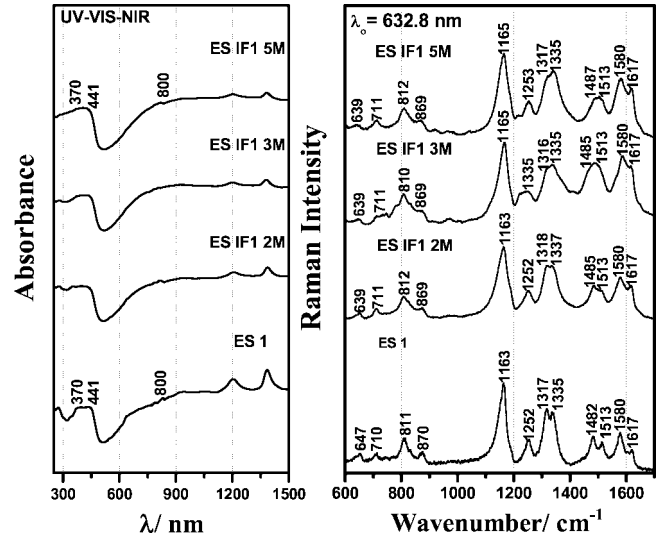

Figure 4. UV-NIS-NIR of powdered samples dispersed in Nujol mineral oil and their RR spectra (from 600 to 1700 cm^{-1}) obtained with laser line at 632.8 nm. The samples are labeled as ES-1M, IF1-2M, IF1-3M, and IF1-5M.

1317−1340 cm^{-1} (νC−N) can be assigned to polaronic units.[33−35] The bands at 1485 cm^{-1} (νC═N) and 1580 cm^{-1} (νC═C) are due to bipolaronic units.[33−35] In addition, the UV−vis-NIR spectra of PANI samples prepared by interfacial route together with PANI in its emeraldine salt are presented in Figure 4. For PANI-ES, the peak at about 440 nm and the broadband starting at about 600−800 nm were assigned to electronic absorptions of radical cation segments.[13] From Figure 4 it was possible to see that the spectra of PANI samples prepared by interfacial route are very similar to PANI-ES spectrum. The UV−vis-NIR data corroborate the Raman data and confirm that all samples are in the emeraldine salt form.

It is well-known that the Raman bands of PANI at wavenumbers higher than 1000 cm^{-1} are sensible to its oxidation and protonation state, but it is difficult to correlate any change to the crystallinity or morphology aspects.[36] Colomban et al.[37] demonstrated that the Raman spectrum of PANI at low wavenumbers is sensible to the kind of crystallinity arrangement of PANI. To verify this trend, the Raman spectra of IF1 samples were obtained at low wavenumbers (see Figure 5). The bands at 200 and 296 cm^{-1} in the Raman spectrum of ES-1M (see Figure 5) was also observed by Colomban et al.[37] According to the authors, these bands owe to the polaronic segments of the PANI with type-I crystalline arrangement[32] (normal modes related to $C_{ring}-N-C_{ring}$ deformation and lattice modes). This assignment is in good agreement with the XRD data (see Figure 2). It is interesting to notice that the intensity of these bands decrease in the Raman spectra of the IF1 samples, being the higher reduction observed for the IF1-5M sample. However, the spectrum of PANI, prepared by the standard procedure[30] using 5.0 mol/L HCl aqueous solution (ES-5M), is similar to the ES-1M. Thus, the effects of HCl concentration over the bands at low wavenumbers (200 and 296 cm^{-1}) is strictly related to IF1 samples. The high acid concentration can promote the increase of the doping degree of PANI (see the doping degree of PANI by the Cl/N ratio in Table 1), but it is reasonable that a part of the HCl (as well the H_2O) is just adsorbed in the PANI particles. Indeed, the nanostructured surface of PANI permits major diffusion of the ions (the higher permeability of the nanostructured PANI was already observed in the literature[38]) inside of the polymeric matrix, leading to a more effective

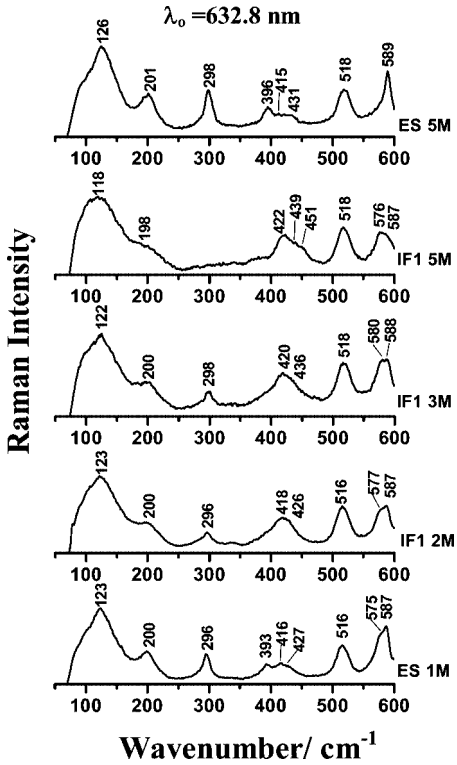

Figure 5. RR spectra (from 50 to 650 cm^{-1}) obtained with laser line at 632.8 nm of powdered samples of ES-1M, IF1-2M, IF1-3M, IF1-5M, and ES-5M. The frequency and intensity values of the band at ca. 120–130 cm^{-1} are changed by the notch filter cutoff.

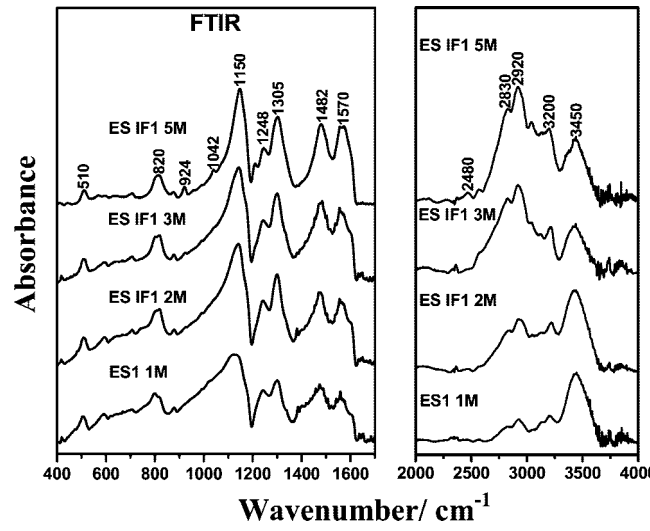

Figure 6. FTIR spectra (baseline corrected) of samples of: ES-1M, IF1-2M, IF1-3M, and IF1-5M in KBr discs.

protonation of the polymeric chain than the PANI prepared in the conventional way.

In addition to the decrease in the intensities of the bands at 200 and 296 cm^{-1}, occur the shift of the bands from 393−427 cm^{-1} for ES-1M sample (see Figure 5) to 422−451 cm^{-1} for IF1-5M (see Figure 5). Cochet et al.,[39−41] in an extensive study about the influence of the conformational changes over the vibrational spectra of PANI, showed that mainly the bands at about 200−500 cm^{-1} are very sensible to the conformational changes. The shift to higher wavenumbers of the bands at about 400 cm^{-1} indicates, according to Cochet et al.,[39−41] the increase of the torsion angles of the $C_{ring}-N-C_{ring}$ segments. Thus, the decrease in the intensities of the bands at 200 and 296 cm^{-1} and also the shift of the bands at about 400 cm^{-1} are due to the conformational changes in the PANI backbone. The increase in the torsion angles is due to the loss of the π-stacking among the PANI rings, leading to the reduction of crystallinity of PANI, as observed in XRD data, and the increase in the higher extension corresponds to the decrease in the amount of nanofibers and increase in regions with irregular morphology in the SEM images of IF1 samples from IF1-2M to IF1-5M.

FTIR spectra of different PANI samples are presented in Figure 6. The samples prepared through interfacial polymerization display similar profile to that observed for PANI prepared by conventional route (ES-1M). The characteristic bands of νC—C stretching vibrations of quinoid (1482 cm^{-1}) and benzenoid (1570 cm^{-1}) segments remain unchanged in all samples, confirming that all samples are in emeraldine salt state, as also clearly verified in UV−vis-NIR and Raman data. The broad absorption band is observed for all FTIR spectra (see the spectra for ES-1M and ES-IF1-5M before the baseline correction in the additional information), this feature is also attributed to the intrachain (free-carrier) excitation.[42] It can be observed, in the region from 900 to 1100 cm^{-1}, an increase of small bands at 924 cm^{-1} and 1042 cm^{-1} from ES-1M to ES-IF1-5M. According to Morales et al.,[43,44] these bands are correlated to the ring-chlorination of aniline or polyaniline that occurs mainly when the polymerization is carried out in medium having high HCl concentration. Small changes in the benzene ring due to the HCl was also observed by Furukawa et al.[33,34] At first glance, we could relate the chlorination with changes in the torsion angles of the $C_{ring}-N-C_{ring}$ observed in the Raman spectra. However, the changes in the region from 2000 to 4000 cm^{-1} is much higher and must be related to the changes observed in the Raman spectra showed in the Figure 5. It is clearly observed that the bands related to NH_2^+ modes at 2480, 2830, and 2920 cm^{-1} increase from ES-1M to ES-IF1-5M, confirming the increase of protonated imine and amine nitrogens in the structure of PANI-ES (see Scheme 1). The bands at about 3200 and 3450 cm^{-1} also change their relative intensities from ES-1M to ES-IF1-5M and these bands are related to N−H stretching modes (evidently there is some contribution of O−H stretching due to the adsorbed water, but the amount of adsorbed water is practically the same for the samples showed in Figure 6, see Table 1). The band at 3200 and 3450 cm^{-1} can be assigned to bonded N−H and free N−H stretching modes,[45,46] showing that the contribution of the different types of hydrogen bonds are also changed by the increase of acidity of the synthetic medium.

Figure 7 shows the EPR spectra of different PANI samples. The decrease of the EPR signal from IF1-2M to IF1-5M can be observed in Figure 7. It is clearly observed that the number of spins (given by double integration) divided by the repeat unit of PANI (tetramer, see Table 1) diminishes from ES-IF1-2M to ES-IF1-5M, confirming the conversion of polaronic segments to spinless structures. Another important aspect is the reduction of the line width (ΔH_{pp}) of the EPR band (see the plot at the bottom of Figure 7) from the ES-1M to IF1-5M. The reduction of the EPR signal can be explained by the conversion of polarons to bipolaron segments, which is the common behavior for heavily doped conducting polymers.[8−10] The increase of the doping degree is corroborated by the Cl/N ratios, see Table 1.

According to the literature, the line width of the EPR band (ΔH_{pp}) is related to the polaron delocalization.[47,48] Conducting polymers typically present a line width from 1 to 10 G. This is due to both delocalization of charge along the polymer chain and to motional narrowing or some type of exchange interac-

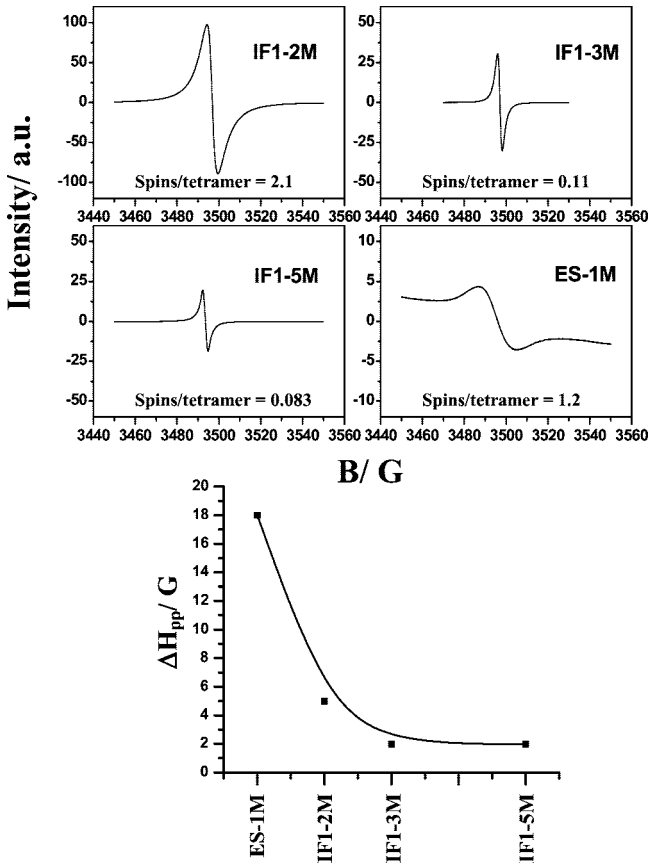

Figure 7. EPR of solid samples of ES-1M, IF1-2M, IF1-3M, and IF1-5M. Inside the figure is given the value of the number of spins (double integration) divided by the tetramer units (see Table 1). (Bottom figure) Plot of ΔH_{pp} as a function of the HCl concentration used in different PANI samples.

tion.[47,49] Thus, the increase of the acid concentration in the preparation of the IF1 samples leads to the formation of bipolaronic segments and increase of the charge delocalization more than for the PANI samples prepared in the standard procedure. In addition, the increase of quinoid segments (bipolarons) in the PANI chains leads to a high torsion angles of the $C_{ring}-N-C_{ring}$ segments. This behavior was also observed in the study about the Raman dispersion of the base forms of the PANI,[50] where the increase of quinoid units in the PANI chains leads to higher torsion angles and is also in agreement with the Raman data of the IF1 samples.

Conclusion

SEM and diffraction data show that high concentrations of HCl solutions used in the preparation of the PANI nanofibers reduce both crystallinity and quality of the nanofibers obtained through interfacial polymerization. The changes in the RR spectra, from 200 to 500 cm^{-1}, the FTIR data, and the EPR data of the PANI nanofibers reveals an increase in the torsion angles of $C_{ring}-N-C_{ring}$ segments, owing to the formation of bipolarons (protonated, spinless units) in the PANI backbone higher than the PANI samples prepared by the conventional route. The nanostructured surface of PANI permits major diffusion of the ions inside the polymeric matrix leading to a more effective protonation of the polymeric chain than the PANI prepared in the conventional way.

Acknowledgment. This work was supported by FAPESP and CNPq (Brazilian agencies) and pró-reitoria de pesquisa da USP (Pos-doc-grant for G.M.d.N.). Postdoctoral Fellowships from FAPESP and CNPq (G.M.d.N.) and PIBIC-CNPq fellowship (P.Y.G.K.) are gratefully acknowledged. The authors would like to thank the National Synchrotron Light Laboratory (LNLS/Brazil) for SAXS measurements, the LME/LNLS for technical support during SEM measurements and Central Analitica-IQUSP for the elemental analysis. The authors are also grateful to Dr. A. M. C. Ferreira for the EPR spectra. Special thanks to my uncle, Mr. William Cogo, and aunt, Mrs. Quita Cogo, for their helpful support during my postdoctoral period at MIT.

Supporting Information Available: Absorbance spectrum for ES IF1-5M and ES1-1M. This material is available free of charge via the Internet at http://pubs.acs.org.

References and Notes

(1) MacDiarmid, A. G.; Epstein, A. J. *J. Chem. Soc., Faraday Trans.* **1989**, *88*, 317–332.
(2) Geniès, E. M.; Boyle, A.; Lapkowski, M.; Tsintavis, C. *Synth. Met.* **1990**, *36*, 139–182.
(3) MacDiarmid, A. G. *Synth. Met.* **2002**, *125*, 11–22.
(4) Carswell, A. D. W.; O'Rear, E. A.; Grady, B. P. *J. Am. Chem. Soc.* **2003**, *125*, 14793–14800.
(5) Yeh, J. M.; Liou, S. J.; Lai, C. Y.; Wu, P. C. *Chem. Mater.* **2001**, *13*, 1131–1136.
(6) Ogurtsov, N. A.; Pud, A. A.; Kamarchik, P.; Shapoval, G. S. *Synth. Met.* **2004**, *143*, 43–47.
(7) MacDiarmid, A. G.; Epstein, A. J. In *Frontiers of Polymers and Advanced Materials*; Prasad, P. N., Ed.; Plenum Press: New York, 1984; p 251.
(8) Brédas, J. L.; Street, G. B. *Acc. Chem. Res.* **1985**, *18*, 309–315.
(9) Huang, W. S.; MacDiarmid, A. G. *Polymer* **1993**, *34*, 1833–1845.
(10) McCall, R. P.; Ginder, J. M.; Leng, J. M.; Ye, H. J.; Manohar, S. K.; Masters, J. G.; Asturias, G. E.; MacDiarmid, A. G.; Epstein, A. J. *Phys. Rev. B* **1990**, *41*, 5202–5213.
(11) Cao, Y.; Smith, P.; Heeger, A. J. *Synth. Met.* **1994**, *48*, 91–97.
(12) Cardin, D. J. *Adv. Mater.* **2002**, *8*, 553–563.
(13) Do Nascimento, G. M.; Landers, R.; Constantino, V. R. L.; Temperini, M. L. A. *Macromolecules* **2004**, *37*, 9373–9385.
(14) Chiou, N.-R.; Epstein, A. J. *Adv. Mater.* **2005**, *17*, 1679–1683.
(15) Wei, Z.; Wan, M. *Adv. Mater.* **2002**, *14*, 1314–1317.
(16) Huang, J.; Kaner, R. B. *J. Am. Chem. Soc.* **2004**, *126*, 851–855.
(17) Hulteen, J. C.; Martin, C. R. *J. Mater. Chem.* **1997**, *7*, 1075–1087.
(18) Martin, C. R.; Van Dyke, L. S.; Cai, Z.; Liang, W. *J. Am. Chem. Soc.* **1990**, *112*, 8976–8977.
(19) Zhang, Z.; Wei, Z.; Wan, M. *Macromolecules* **2002**, *35*, 5937–5942.
(20) Qiu, H.; Wan, M.; Matthews, B.; Dai, L. *Macromolecules* **2001**, *34*, 675–677.
(21) Wei, Z.; Zhang, Z.; Wan, M. *Langmuir* **2002**, *18*, 917–921.
(22) Do Nascimento, G. M.; Silva, C. H. B.; Temperini, M. L. A. *Macromol. Rapid Commun.* **2006**, *27*, 255–259.
(23) do Nascimento, G. M.; Silva, C. H. B.; Temperini, M. L. A. *Polym. Degrad. Stab.* **2007**, *92*, 1–7.
(24) Gao, H.; Jiang, T.; Han, B.; Wang, Y.; Du, J.; Liu, Z.; Zhang, J. *Polymer* **2004**, *45*, 3017–3019.
(25) Rodrigues, F.; Do Nascimento, G. M.; Santos, P. S. *Macromol. Rapid Commun.* **2007**, *28*, 666–669.
(26) Huang, J.; Kaner, R. B. *Angew. Chem., Int. Ed.* **2004**, *43*, 5817–5821.
(27) Huang, J.; Virji, S.; Weiller, B. H.; Kaner, R. B. *J. Am. Chem. Soc.* **2003**, *125*, 314–315.
(28) Zhang, X.; Goux, W. J.; Manohar, S. K. *J. Am. Chem. Soc.* **2004**, *126*, 4502–4503.
(29) Zhang, X.; Manohar, S. K. *Chem. Commun.* **2004**, *4*, 2360–2361.
(30) MacDiarmid, A. G.; Chiang, J. C.; Richter, A. F., Sonosiri, N. L. D. In *Conducting Polymers*; Alcácer, L., Ed.; Reidel Publications: Dordrecht, Germany, 1987; p 105.
(31) Cavalcanti, L. P.; Kellermann, G.; Plivelic, T.; Neuenschwander, R.; Torriani, I. L. *Activity Report/National Synchrotron Light Laboratory (1997/98)*; Brazilian Association for Synchrotron Light Technology: Campinas, SP, 1997; p 5.
(32) Pouget, J. P.; Jozefowicz, M. E.; Epstein, A. J.; Tang, X.; MacDiarmid, A. G. *Macromolecules* **1991**, *24*, 779–789.
(33) Furukawa, Y.; Ueda, F.; Hyodo, Y.; Harada, I.; Nakajima, T.; Kawagoe, T. *Macromolecules* **1988**, *21*, 1297–1305.
(34) Furukawa, Y.; Hara, T.; Hyodo, Y.; Harada, I. *Synth. Met.* **1986**, *16*, 189–198.

(35) Louarn, G.; Lapkowski, M.; Quillard, S.; Pron, A.; Buisson, J. P.; Lefrant, S. *J. Phys. Chem.* **1996**, *100*, 6998–7006.
(36) Tagowska, M.; Pałys, B.; Jackowska, K. *Synth. Met.* **2004**, *142*, 223–229.
(37) Colomban, Ph.; Folch, S.; Gruger, A. *Macromolecules* **1999**, *32*, 3080–3092.
(38) Sukeerthi, S.; Contractor, A. Q. *Anal. Chem.* **1999**, *71*, 2231–2236.
(39) Cochet-Landrieau, M. Ph.D. Thesis, Université de Nantes, Nantes, France, 1999.
(40) Cochet, M.; Louarn, G.; Quillard, S.; Boyer, M. I.; Buisson, J. P.; Lefrant, S. *J. Raman Spectrosc.* **2000**, *31*, 1029–1039.
(41) Cochet, M.; Louarn, G.; Quillard, S.; Buisson, J. P.; Lefrant, S. *J. Raman Spectrosc.* **2000**, *31*, 1041–1049.
(42) Ping, Z. *J. Chem. Soc., Faraday Trans.* **1996**, *92*, 3063–3067.
(43) Morales, G. M.; Llusa, M.; Miras, M. C.; Barbero, C. *Polymer* **1997**, *38*, 5247–5250.
(44) Morales, G. M.; Miras, M. C.; Barbero, C. *Synth. Met.* **1999**, *101*, 687.
(45) Jana, T.; Roy, S.; Nandi, A. K. *Synth. Met.* **2003**, *132*, 257.
(46) Lunzy, W.; Banka, E. *Macromolecules* **2000**, *33*, 425.
(47) Yang, S. M.; Lin, T. S. *Synth. Met.* **1989**, *29*, E227–E234.
(48) Monkman, A. P.; Bloor, D.; Stevens, G. C. *J. Phys. D: Appl. Phys.* **1990**, *23*, 627–629.
(49) Scott, J. C.; Pflunger, P.; Krounbi, M. T.; Street, G. B. *Phys. Rev. B* **1983**, *28*, 2140–2145.
(50) do Nascimento, G. M.; Kobata, P. Y. G.; Millen, R. P.; Temperini, M. L.A. *Synth. Met.* **2007**, *157*, 247–251.

JP804154K